

# Exploring the conformal transition from above and below

Alex Pomarol<sup>a,b</sup> and Lindber Salas<sup>a,b</sup>

<sup>a</sup>*IFAE and BIST, Universitat Autònoma de Barcelona, 08193 Bellaterra, Barcelona*

<sup>b</sup>*Dept. de Física, Universitat Autònoma de Barcelona, 08193 Bellaterra, Barcelona*

## Abstract

We consider conformal transitions arising from the merging of IR and UV fixed points, expected to occur in QCD with a large enough number of flavors. We study the smoothness of physical quantities across this transition, being mostly determined by the logarithmic breaking of conformal invariance. We investigate this explicitly using holography where approaching the conformal transition either from outside or inside the conformal window (perturbed by a mass term) is characterized by the same dynamics. The mass of spin-1 mesons and  $F_\pi$  are shown to be continuous across the transition, as well as the dilaton mass. This implies that the lightness of the dilaton cannot be a consequence of the spontaneous breaking of scale invariance when leaving the conformal window. Our analysis suggests that the light scalar observed in QCD lattice simulations is a  $q\bar{q}$  meson that becomes light since the  $q\bar{q}$ -operator dimension reaches its minimal value.

# 1 Introduction

A conformal field theory (CFT) can depart from its IR fixed point in various way as we vary the parameters of the model. Either because the IR fixed point goes to zero, to infinity or it merges with a UV fixed point. We are interested in conformal transitions characterized by this third case, the merging of the IR fixed point with a UV fixed point.

It has been speculated [1] that this is the case for  $SU(N_c)$  gauge theories as QCD at the lower edge of the conformal window –see Fig. 1. As we decrease the number of flavors  $N_F$  from the Banks-Zaks fixed point at  $N_F = \frac{11}{2}N_c$ , where QCD enters into the conformal window, to some critical value  $N_F = N_F^{crit}$ , QCD is expected to loose conformality by an IR-UV fixed point merging. Interestingly, in the last years lattice simulations have been providing abundant data on the properties of QCD at different values of  $N_F$  and quark masses  $M_q$ , helping to better understand this conformal transition [2, 3, 4, 5]. A particularly intriguing feature is the presence of a very light  $0^{++}$  state when QCD is close to (but outside) the conformal transition. It has been speculated that this state could be a dilaton, the Goldstone associated to the spontaneous breaking of scale invariance.

We will consider CFTs in the large- $N_c$  limit. It has been argued in [6, 7] that when these models are close to the conformal transition, they must contain a scalar operator  $\mathcal{O}_\Phi$  whose dimension gets close to 2, becoming imaginary when leaving the conformal window. For QCD, where in the large- $N_c$  limit  $N_F^{crit}/N_c \equiv x_{crit}$  becomes a continuous parameter,  $\mathcal{O}_\Phi$  corresponds to the  $q\bar{q}$  operator.

We are interested in understanding how the physical quantities change as we move across the conformal transition.<sup>1</sup> Using holography [10] we will show how the meson mass spectrum is mostly dictated by chiral and conformal invariance and the way this is broken. We will show that spin-1 meson masses and  $F_\pi$  are continuous across the transition, while the masses of the scalar mesons,  $f_0$  and  $a_0$ , show a jump due to a logarithmic breaking of conformal invariance.

The mass of the dilaton, corresponding to a glueball, is also found to be smooth across the transition, implying that this must be light at both sides of the conformal window. This implies that the lightness of the dilaton cannot only be a consequence of the spontaneous breaking of the conformal symmetry when leaving the conformal window. We will argue that this disfavors this state as the light  $0^{++}$  scalar found in lattice simulations.

On the other hand, we will consider the possibility that the lightness of the  $0^{++}$  scalar found in lattice simulations is a  $q\bar{q}$  meson whose mass is small due to the fact that  $\text{Dim}[\mathcal{O}_\Phi] \rightarrow 2$  at the conformal edge. This is the closest value to the unitary bound  $\text{Dim}[\mathcal{O}_\Phi] \geq 1$  where a scalar is expected to become massless since the operator  $\mathcal{O}_\Phi$  decouples from the CFT [11]. We will also understand why the breaking of the chiral symmetry is smaller as we move inside the conformal window, as lattice simulations seem to suggest.

---

<sup>1</sup>Effective field theories (EFTs) for a light dilaton have been widely developed [8, 9]. Nevertheless, these are limited to small  $M_q$  values and cannot be used to describe the conformal transition.

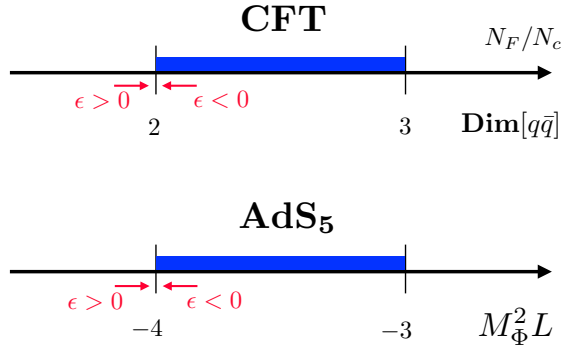


Figure 1: *QCD conformal window and the holographic equivalent.*

Although some of these properties could also be derived following 4D CFT approaches, for example in [12] or [13], we will see that it is much easier to derive them using holography.

## 2 Conformal transition by fixed-point merging

Following [1], we will consider that the conformal transition occurs when an IR fixed point merges with a UV fixed point. For theories at large- $N_c$ , it can be shown [6, 7] that close to the transition the theories must have a marginal operator  $\mathcal{O}_f$

$$f(\mu)\mathcal{O}_f \in \mathcal{L}, \quad (1)$$

whose coupling  $f$  has a beta function given by

$$\beta_f \simeq \epsilon + (f - f_*)^2. \quad (2)$$

For  $\epsilon < 0$  this beta function has two zeros corresponding to an IR and a UV fixed point that merge to a single fixed point at  $\epsilon = 0$ , that disappears for  $\epsilon > 0$ . This marks the conformal transition. In QCD we expect  $\epsilon \propto x_{crit} - x$ .

Therefore, as we approach the conformal transition ( $\epsilon \rightarrow 0$ ), the theory can be in two different phases depending on the sign of  $\epsilon$ :

- For  $\epsilon < 0$ , Eq. (2) gives us

$$f(\mu) \simeq f_* - \frac{1}{\ln \mu/\mu_0}, \quad (3)$$

and  $f$  will run towards the IR,  $\mu/\mu_0 \rightarrow 0$ , approaching  $f_*$  where the theory becomes conformal,  $\beta_f \rightarrow 0$ . Here  $\mu_0$  is an arbitrary scale related with the value of  $f$  at the UV.

- For  $\epsilon > 0$ , there are no possible zeros for  $\beta_f$ . In this case, we have

$$f(\mu) \simeq f_* + \sqrt{\epsilon} \tan \left( \sqrt{\epsilon} \ln \frac{\mu}{\mu_0} \right), \quad (4)$$

and  $f(\mu)$  runs slowly when  $f \sim f_*$ , behaving almost as a CFT, but it blows up at some IR scale  $\mu_{\text{IR}}$  determined by

$$\sqrt{\epsilon} \ln \frac{\mu_{\text{IR}}}{\mu_0} \simeq -\frac{\pi}{2}. \quad (5)$$

Therefore conformality is never reached. In fact, the dimension of  $\mathcal{O}_f$ , formally given by

$$\text{Dim}[\mathcal{O}_f] = 4 + \frac{d\beta_f}{df} \simeq 4 + 2\sqrt{-\epsilon}, \quad (6)$$

becomes complex for  $\epsilon > 0$ .

These two phases corresponds to the two sides of the conformal lower edge shown in Fig. 1.

It has also been shown in [6, 7] that for theories in the large- $N_c$  limit,  $\mathcal{O}_f$  must be a double-trace operator, made of the squared of a single-trace operator  $\mathcal{O}_\Phi$ , i.e.,  $\mathcal{O}_f = |\mathcal{O}_\Phi|^2$ . Since in the large  $N_c$ ,  $\text{Dim}[\mathcal{O}_f] = 2\text{Dim}[\mathcal{O}_\Phi]$ , we have from Eq. (6)

$$\text{Dim}[\mathcal{O}_\Phi] = 2 + \sqrt{-\epsilon}. \quad (7)$$

In QCD, as argued in [1],  $\mathcal{O}_\Phi$  is expected to be the operator made of quarks,  $q\bar{q}$ , whose dimension will go from  $\sim 3$  when entering the conformal window at the upper edge to 2 at the lower edge (see Fig. 1). The fact that  $\mathcal{O}_\Phi$  reaches the lowest dimension at the conformal transition can explain the existence of a relative light scalar meson (with respect to the vector one,  $m_\rho$ ) [14]. Indeed,  $\text{Dim}[\mathcal{O}_\Phi]$  gets at the edge of the conformal transition the closest value to  $\text{Dim}[\mathcal{O}_\Phi] = 1$  (unitarity bound) at which the scalar operator decouples from the CFT [11], becoming then insensitive to the CFT IR scale.

All the above properties of this conformal transition find a beautiful implementation in holographic models by the use of the correspondence (or duality) between strongly-coupled  $\text{CFT}_4$  (in the large  $N_c$  and large 'tHooft coupling<sup>2</sup>) and weakly-coupled five-dimensional Anti-de-Sitter theories ( $\text{AdS}_5$ ) [10]. Operators in the  $\text{CFT}_4$  ( $\mathcal{O}_\Phi$ ) correspond to scalar fields in the  $\text{AdS}_5$  ( $\Phi$ ) where dimensions and masses are related via the the AdS/CFT relation [10]:

$$\text{Dim}[\mathcal{O}_\Phi] = 2 + \sqrt{4 + M_\Phi^2 L^2}. \quad (8)$$

Eq. (8) tells us that the conformal transition must occurs when the 5D scalar mass  $M_\Phi^2 L^2$  becomes smaller than  $-4$  (see Fig. 1). Indeed, in this case the mass is below the Breitenlohner-Freedman (BF) bound that determines the stability of a scalar in  $\text{AdS}_5$ . For  $M_\Phi^2 < -4/L^2$  the scalar  $\Phi$  becomes tachyonic, turning on in the 5D bulk [17, 14].<sup>3</sup>

<sup>2</sup>It has been recently shown [15, 16] that higher spin decouple from low-energy observables, making holography a good approach even for models where the 'tHooft coupling is not very large.

<sup>3</sup>Alternatively, one could consider holographic models of complex CFTs, as done in [18].

## 2.1 Probing the conformal phase by $M_q \mathcal{O}_\Phi$

We are interested in understanding the properties of the mass spectrum at the two sides of the conformal edge. Since the spectrum in the conformal phase is continuous, we will perturb the theory by adding to the Lagrangian the term

$$\Delta\mathcal{L} = M_q \mathcal{O}_\Phi \quad (M_q \geq 0), \quad (9)$$

that explicitly breaks scale invariance. In QCD this corresponds to add a mass to the quarks,  $M_q q\bar{q}$ , that not only breaks conformal invariance but also the chiral symmetry; this is also done in lattice simulations.

A nonzero  $M_q$  allows to probe the physical properties of the theory inside the conformal window, as the mass spectrum becomes discrete and can be compared with the one at the other side of the edge of the transition. All the masses are expected to be proportional to  $M_q^{1/(4-\text{Dim}[\mathcal{O}_\Phi])}$ , referred as "hyperscaling". At the conformal edge where  $\text{Dim}[\mathcal{O}_\Phi] \rightarrow 2$ , we then have

$$m_i = a_i \sqrt{M_q}, \quad (10)$$

where  $a_i$  are parameters that depend on the details of the model. Obviously, the ratio of masses is independent of  $M_q$ .

The presence of  $M_q$  in the conformal theory ( $\epsilon < 0$ ) brings also a logarithmic divergence that can be easily understood from scale invariance [19]. Since  $\text{dim}[\mathcal{O}_\Phi] \rightarrow 2$ , the two-point function in momentum space is given by

$$\int d^4x e^{ip \cdot x} \langle \mathcal{O}_\Phi(x) \mathcal{O}_\Phi(0) \rangle \sim \int d^4x \frac{1}{|x|^4} \sim \ln \Lambda. \quad (11)$$

Therefore we expect a logarithmic breaking of conformal invariance in  $\langle \mathcal{O}_\Phi \rangle$  proportional to  $M_q$ . Notice however that  $M_q$  does not enter into the log, so Eq. (10) is always guaranteed.

From outside the conformal window ( $\epsilon > 0$ ), the situation is different. If we add Eq. (9) and increase  $M_q$  over the scale  $\mu_{\text{IR}}$  defined in Eq. (5), the coupling  $f(\mu)$  stays almost constant around  $f_*$  as in a CFT. Therefore in the limit  $M_q \gg \mu_{\text{IR}}$  the mass spectrum must smoothly tend to Eq. (10).

Before moving to the holographic model, we must remark that our analysis using holography shares many features of that in [12] based on the Schwinger-Dyson equation for the renormalized fermion self-energy. It is also related to the approach taken in [13] where the theory is assumed to be conformal deep in the IR.

## 3 A five-dimensional model for the conformal transition

A holographic model with the properties of described above was presented in [14] (for other models, see [17, 20]). This consists in a  $SU(N_F)_L \otimes SU(N_F)_R$  gauge theory in 5D with a

complex scalar  $\Phi$  transforming as a  $(\mathbf{N}_F, \overline{\mathbf{N}}_F)$ .<sup>4</sup> This scalar plays the role of the  $q\bar{q}$  operator in 4D QCD. Imposing parity ( $L \leftrightarrow R$ ), the action is given by

$$S_5 = \int d^4x \int dz \sqrt{g} M_5 \left[ \frac{1}{\kappa^2} (\mathcal{R} + \Lambda_5) + \mathcal{L}_5 \right], \quad (12)$$

where the Lagrangian is given by

$$\mathcal{L}_5 = -\frac{1}{4} \text{Tr} [L_{MN} L^{MN} + R_{MN} R^{MN}] + \frac{1}{2} \text{Tr} |D_M \Phi|^2 - V_\Phi(\Phi), \quad (13)$$

with  $L_{MN}$ ,  $R_{MN}$  being the field-strength of the  $SU(N_F)_L$  and  $SU(N_F)_R$  gauge bosons respectively, and the indices run over the five dimensions,  $M = \{\mu, 5\}$ . We parametrize the fields as  $\Phi = \Phi_s + T_a \Phi_a$  with  $\text{Tr}[T_a T_b] = \delta_{ab}$ . The fields  $\Phi_s$  and  $\Phi_a$  will respectively transform as singlet and adjoint under  $SU(N_F)_V$ , the remaining symmetry after  $\Phi \neq 0$  breaks the chiral symmetry. The covariant derivative is defined as

$$D_M \Phi = \partial_M \Phi + ig_5 L_M \Phi - ig_5 \Phi R_M, \quad (14)$$

and the potential is given by<sup>5</sup>

$$V_\Phi(\Phi) = \frac{1}{2} M_\Phi^2 \text{Tr} |\Phi|^2 + \frac{1}{4} \lambda_1 \text{Tr} |\Phi|^4 + \frac{1}{4} \lambda_2 (\text{Tr} |\Phi|^2)^2. \quad (15)$$

The 5D metric in conformal coordinates is defined as

$$ds^2 = a(z)^2 (\eta_{\mu\nu} dx^\mu dx^\nu - dz^2), \quad (16)$$

where  $\eta_{\mu\nu} = \text{diag}(1, -1, -1, -1)$  and  $a(z)$  is the warp factor. Before the scalar  $\Phi$  turns on, the presence of  $\Lambda_5$  leads to an  $\text{AdS}_5$  geometry:

$$a(z) = \frac{L}{z}, \quad (17)$$

where  $L^2 = 12/\Lambda_5$  is the squared AdS curvature radius. The 5D space will be cut off by an IR-brane at some point  $z = z_{\text{IR}}$  to be determined dynamically. Also a UV-boundary at  $z = z_{\text{UV}}$  will be needed to regularize the theory. The limit  $z_{\text{UV}} \rightarrow 0$  will be taken in a proper way to provide finite physical quantities [10].

The dimension of  $\mathcal{O}_\Phi$ , Eq. (7), is related by Eq. (8) to the 5D mass of  $\Phi$ :

$$M_\Phi^2 = -\frac{4 + \epsilon}{L^2}. \quad (18)$$

When  $\epsilon < 0$  the mass of  $\Phi$  is above the BF bound and  $\Phi$  does not turn on, as we will see in Sec. 3.1.2. Nevertheless, for  $\epsilon > 0$  the mass is below the BF bound and  $\Phi$  turns on in the 5D bulk [14], breaking the conformal and chiral symmetry. Therefore, as in the strongly-coupled model described in Sec. 2, we have two phases separated by the sign of  $\epsilon$  (see Fig. 1):

<sup>4</sup>With respect to [14], we are neglecting the  $U(1)_B$  gauge sector that does not play any role in the discussion.

<sup>5</sup>We notice that one can absorb one coupling into  $M_5$ , as we will do later –see footnote 6.

- $\epsilon > 0 \Rightarrow$  non-AdS<sub>5</sub> (non-CFT<sub>4</sub>) phase.
- $\epsilon < 0 \Rightarrow$  AdS<sub>5</sub> (CFT<sub>4</sub>) phase.

The presence of the IR-brane add extra parameters to the theory as  $\Phi$  might also have a potential on the IR-boundary. Following the EFT criteria of [14], we have

$$\mathcal{L}_{\text{IR}} = -a^4 \tilde{V}_b(\Phi)|_{z_{\text{IR}}}, \quad \tilde{V}_b(\Phi) = \frac{\Lambda_4}{\kappa^2} + \frac{1}{2} m_b^2 \text{Tr} |\Phi|^2. \quad (19)$$

### 3.1 The $\phi(z)$ profile

The conformal and the chiral symmetry breaking  $SU(N_F)_L \otimes SU(N_F)_R \rightarrow SU(N_F)_V$  is trigger by a nonzero profile for  $\phi = \text{Tr}|\Phi|$ . From Eq. (13), the equation of motion for  $\phi$  is determined to be

$$-\frac{1}{a^5} (\partial_5 a^3 \partial_5 - a^3 \partial^\mu \partial_\mu) \phi + M_\Phi^2 \phi + \lambda \phi^3 = 0, \quad (20)$$

where  $\lambda \equiv \lambda_1 + N_F \lambda_2$  and the warp factor is determined by the Einstein equations [14]:

$$-\frac{\dot{a}}{a^2} = \sqrt{\frac{1}{L^2} + \frac{\hat{\kappa}^2 L^2}{12} \left( \frac{\dot{\phi}^2}{2a^2} - V(\phi) \right)}, \quad (21)$$

with  $\dot{\phi} \equiv \partial_z \phi$  and  $\hat{\kappa}^2$  being the 5D gravitational strength. The boundary conditions are the following. At the UV-boundary we fix

$$L\phi|_{z_{\text{UV}}} = z_{\text{UV}}^2 M_q. \quad (22)$$

$M_q$  plays the role of the quark mass in the dual gauge theory, Eq. (9). It has dimension

$$\text{Dim}[M_q] = 4 - \text{Dim}[\mathcal{O}_\Phi], \quad (23)$$

so at the conformal edge we have  $\text{Dim}[M_q] \rightarrow 2$ . For  $M_q \neq 0$ ,  $\phi$  turns on independently of the sign of  $\epsilon$ , and the conformal and chiral symmetry are broken inside the 5D bulk. For  $M_q = 0$ , the field  $\phi(z)$  gets a nonzero profile only when we are outside the conformal window ( $\epsilon > 0$ ), as we will explicitly see later. At the IR-brane we must impose the boundary condition determined by the model. We have [14]

$$\left( \frac{M_5}{a} \dot{\phi} + \partial_\phi V_b \right) \Big|_{z_{\text{IR}}} = 0, \quad \left( -\frac{6M_5}{\hat{\kappa}^2 L^2} \frac{\dot{a}}{a^2} + V_b \right) \Big|_{z_{\text{IR}}} = 0. \quad (24)$$

The first one is the IR condition for  $\phi$ , while the second one is the junction condition that determines the position of the IR-brane  $z_{\text{IR}}$ .

Although we will present in the next section results with no approximations, it is instructive to consider the case in which the profile of  $\phi$  can be solved analytically. For this, we will take

the approximation that  $\phi$  is small such that the quartic term can be neglected as well as the feedback of  $\phi$  on the metric, i.e., the 5D space is AdS<sub>5</sub>. Eq. (24) reduces in this case to

$$\dot{\phi}(z_{\text{IR}}) = -\frac{m_b^2 L}{z_{\text{IR}} M_5} \phi_{\text{IR}}, \quad \phi(z_{\text{IR}}) = \phi_{\text{IR}}, \quad (25)$$

where we have introduced the parameter  $\phi_{\text{IR}}$  related to other parameters of the model (a combination of  $\hat{\kappa}^2$ ,  $m_b^2$ ,  $\Lambda_4$  and the sign of  $\lambda$  [14]).<sup>6</sup> We will restrict to  $m_b^2 > -2M_5/L$  that guarantees that the conformal symmetry is not broken by the IR-boundary potential.

### 3.1.1 Towards the conformal transition from outside ( $\epsilon > 0$ )

With the above approximations, we can solve  $\phi$  analytically. For  $\epsilon > 0$ , the two solutions are  $z^{2 \pm i\sqrt{\epsilon}}$  that we can write as

$$\phi(z) = \frac{A}{L^3} z^2 \sin\left(\sqrt{\epsilon} \ln \frac{z}{z_{\text{UV}}} + \beta\right), \quad (26)$$

where  $A$  and  $\beta$  are dimensionless constants to be determined by the boundary conditions. From Eq. (22) and Eq. (24), we get

$$M_q = \frac{A}{L^2} \sin \beta, \quad (27)$$

and

$$\tan\left(\sqrt{\epsilon} \ln \frac{z_{\text{IR}}}{z_{\text{UV}}} + \beta\right) = -\frac{\sqrt{\epsilon}}{\tilde{m}_b^2}, \quad (28)$$

where  $\tilde{m}_b^2 \equiv 2 + m_b^2 L/M_5$ . In the limit  $\epsilon \rightarrow 0$ , Eq. (28) tells us that  $\sin(\sqrt{\epsilon} \ln z_{\text{IR}}/z_{\text{UV}} + \beta) \rightarrow \sqrt{\epsilon}$ . Therefore expanding Eq. (28) around  $z_c$  determined by<sup>7</sup>

$$\sqrt{\epsilon} \ln \frac{z_c}{z_{\text{UV}}} + \beta = n\pi, \quad n = 1, 2, \dots, \quad (29)$$

we get

$$\ln \frac{z_{\text{IR}}}{z_c} = -\frac{1}{\tilde{m}_b^2} < 0. \quad (30)$$

Notice that the limit  $\epsilon \rightarrow 0$  must be taken with  $z_{\text{UV}} \rightarrow 0$  according to Eq. (29). Using Eq. (25) and Eq. (30) we finally get

$$\phi(z) = -\phi_{\text{IR}} \tilde{m}_b^2 \left(\frac{z}{z_{\text{IR}}}\right)^2 \ln \frac{z}{a z_{\text{IR}}}, \quad (31)$$

where  $a = \text{Exp}[1/\tilde{m}_b^2]$ . It is interesting to remark that Eq. (31) is valid for any value of  $M_q$ . In the particular case  $M_q = 0$ , we have from Eq. (27) that  $\beta = 0$  but  $A \neq 0$ , corresponding to a spontaneous breaking of the conformal and chiral symmetry.

<sup>6</sup> By field redefinitions we can absorb  $|\lambda|$  in other parameters. Therefore, with no loss of generality, we can consider  $\lambda = \pm 1$ .

<sup>7</sup>The solution for  $n = 1$  corresponds to a global minimum, while  $n > 1$  just gives local minima (corresponding to a surviving discrete conformal invariance).



The above is in accordance with the discussion in Sec. 2 where for  $\epsilon > 0$  it was shown that  $f(\mu)$  runs as Eq. (4) and diverges at the scale  $\mu_{\text{IR}} \sim 1/z_c$  for  $\mu_0 \sim \text{Exp}[-\pi/(2\sqrt{\epsilon})]/z_{\text{UV}}$ .

### 3.1.2 Towards the conformal transition from inside ( $\epsilon < 0$ )

Let us now consider the solution of  $\phi$  from the other side of the conformal edge,  $\epsilon < 0$ . In this case the two possible solutions are  $z^{2\pm\sqrt{|\epsilon|}}$  that in the limit  $\epsilon \rightarrow 0$  leads to  $z^2$  and  $z^2 \ln z$ . We can then write the most general solution as

$$\phi = \frac{z^2}{L^3} \hat{A} \ln \frac{z}{z_0}, \quad (32)$$

where  $\hat{A}$  and  $z_0$  are the two parameters to be fixed by the boundary conditions. Eq. (22) gives

$$M_q = \frac{\hat{A}}{L^2} \ln \frac{z_{\text{UV}}}{z_0}. \quad (33)$$

From the IR-brane boundary conditions we get, similarly to Eq. (30),

$$\ln \frac{z_{\text{IR}}}{z_0} = -\frac{1}{\tilde{m}_b^2} < 0, \quad (34)$$

that leads exactly to Eq. (31). We notice however an important difference in this case with respect to the  $\epsilon > 0$  case. From Eq. (33) we have that  $M_q = 0$  requires  $z_0 \rightarrow z_{\text{UV}}$ , but this is incompatible with Eq. (34). In other words, there is no nonzero solution for  $\phi$  when  $M_q = 0$ . As expected, the model flows to the conformal phase for  $M_q = 0$ .

We can then conclude from the above analysis that approaching the conformal transition  $\epsilon \rightarrow 0$  from inside the conformal window ( $\epsilon < 0$ ) or outside ( $\epsilon > 0$ ) gives the same profile for  $\phi$  (Eq. (31)) and, as a consequence, the spontaneous conformal and chiral breaking driven by  $\phi$  at the IR have to be felt equally in both sides of the transition, independently of the value of  $M_q \neq 0$ .

## 4 Mass spectrum

Let us discuss here what differences we expect in the mass spectrum of the theory when we approach the conformal edge from inside or outside the conformal window. We will back up our arguments with the mass spectrum calculated in the holographic model with no approximations. For the numerical analysis we will take the benchmark values

$$\phi_{\text{IR}} = 1, \quad \lambda = 1, \quad N_F \lambda_2 = -2, \quad \tilde{m}_b^2 = 1, \quad \hat{\kappa} = 1, \quad g_5 = 1.52. \quad (35)$$

The mass spectrum would change by varying these values, but the qualitative picture will be the same. For other values of the parameter space see [14].

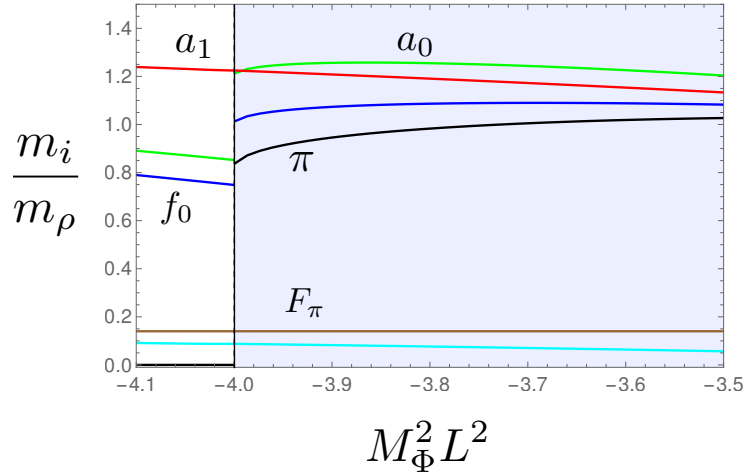


Figure 2: Mass spectrum of mesons, normalized to  $m_\rho$ , as a function of the 5D scalar mass or equivalently  $\text{Dim}[q\bar{q}]$  defined in Eq. (8). The values of the model are given in Eq. (35). We vary the value of  $\phi_{\text{IR}}$  to keep  $F_\pi/m_\rho$  fixed. The sky-blue line corresponds to the dilaton/radion (glueball). For  $M_\Phi^2 L^2 < -4$  we have  $M_q = 0$ , while for  $M_\Phi^2 L^2 > -4$  we have  $M_q \neq 0$ .

#### 4.1 Spin-1 states

It is clear that vector states, coming from the Kaluza-Klein (KK) decomposition of  $V_M = (L_M + R_M)/\sqrt{2}$  are not much affected by the scalar  $\phi(z)$  since they do not couple to it. They can only notice a nonzero  $\phi$  from the feedback of this on the metric. This clearly affects the KK spectrum, but this is expected to be quite universal for the different type of states. For this reason, we will use the mass of the lightest vector state, the  $\rho$ , to normalize the other masses.

The axial-vector  $A_M = (L_M - R_M)/\sqrt{2}$  couple to  $\phi$  through the covariant derivative, and therefore a nonzero  $\phi$  splits the masses of the KK of  $A_M$  from those of  $V_M$ . Since  $\phi$  has the same profile at both sides of the conformal edge independently of  $M_q$ , as shown in Eq. (31), we expect the masses of the axial-vectors to be smooth across the transition. Similarly for  $F_\pi$ , defined as the axial-vector two-point correlator at zero momentum [14], we expect this quantity to be independent of  $M_q$  and smooth across the transition.

In Fig. 2 we show the mass of the lightest axial-vector,  $a_1$  as well as  $F_\pi$  normalized to  $m_\rho$ . We indeed see that these values are smooth across the transition. To show that these physical quantities are also independent of  $M_q$ , we plot in Fig. 3 the predictions of the holographic model as a function of  $M_q$  for  $\epsilon > 0$ . We remark again that this is obvious for  $\epsilon < 0$  (hyperscaling) but not for  $\epsilon > 0$ . Indeed we see in Fig. 3 that  $a_1$  and  $F_\pi$  (normalized to  $m_\rho$ ) do not vary as we move  $M_q$ .

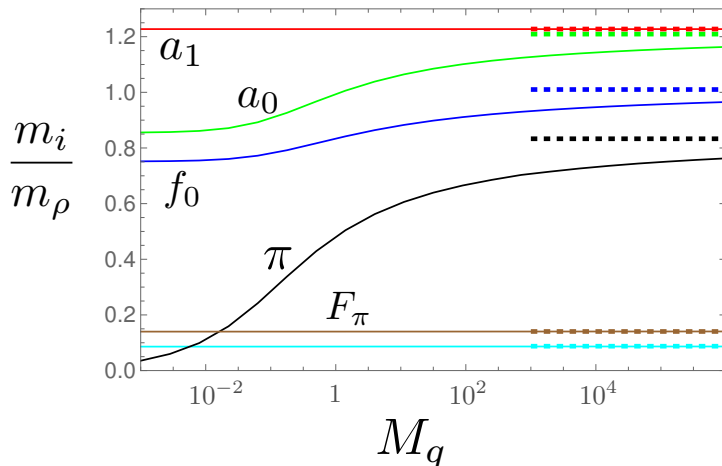


Figure 3: Mass spectrum of mesons outside the conformal window  $\epsilon > 0$ , normalized the  $m_\rho$ , as a function of  $M_q$ . In dashed-lines the values for  $\epsilon < 0$ . The sky-blue line corresponds to the dilaton/radion (glueball).

## 4.2 The dilaton/radion

It has been claimed that approaching the conformal edge from below, the theory could have a light scalar, the dilaton, associated to the spontaneous breaking of the conformal invariance. This has been partly supported by lattice results [2, 3, 4] that have seen a  $0^{++}$  state below the  $\rho$  mass for values of  $N_F$  where one expects to be outside (but close to) the conformal window. In [14] it was shown that in holographic models the radion, that corresponds to the dilaton in the 4D dual theory, was the lightest state of the spectrum, although not parametrically lighter than the others (see also [17, 20]). This state arises from the KK decomposition of the  $\text{AdS}_5$  gravitons, and therefore should be considered a glueball state (it mixes with the mesons from  $\Phi$  but the mixing comes out to be small [14]).

Since we showed that the profile of  $\phi$  is the same at both sides of the conformal transition, we must also expect a light radion/dilaton inside the conformal window (for  $M_q \neq 0$ ) as long as we are close to the lower edge. We find that this is indeed the case. As it can be appreciated in Fig. 2 the radion/dilaton mass is smooth across the transition and is also light inside the conformal window. The reason for this lightness can be found in [14] since the argument given there can also be applied at the other side of the transition (for  $\epsilon < 0$ ). This surprising result shows that this light dilaton has nothing to do with the spontaneous breaking of the conformal symmetry.

Another important property of the radion/dilaton is that its mass (normalized to  $m_\rho$ ) is practically independent of  $M_q$ , since the profile of  $\phi$ , given in Eq. (31), is the same for any value of  $M_q$ . This is shown in Fig. 3 by a sky-blue line.

### 4.3 Scalar mesons

Let us now analyze the mass spectrum of the fluctuations of  $\Phi$  corresponding to  $q\bar{q}$  mesons. Although they can in principle mix with the glueballs, we find that in our holographic model this mixing is small. Let us start with the radial excitations and consider later the angular fluctuations corresponding to the Goldstones.

#### 4.3.1 Radial fluctuations: $0^{++}$ states

To understand the dependence on the sign of  $\epsilon$ , we will first calculate the scalar-scalar correlator on the  $\text{AdS}_5$  boundary at  $z = z_{\text{UV}} \rightarrow 0$ . To obtain analytical expressions, we will work in the approximation where the quartic couplings and the feedback on the metric are neglected. At this level the singlet and adjoint scalars are degenerate. Following [21], we have (neglecting an overall factor)

$$\Pi_S(p) = M_5 L \left[ 2 + z_{\text{UV}} \frac{\partial_z J_{\sqrt{-\epsilon}}(ipz) + b(p) \partial_z Y_{\sqrt{-\epsilon}}(ipz)}{J_{\sqrt{-\epsilon}}(ipz) + b(p) Y_{\sqrt{-\epsilon}}(ipz)} \right]_{z=z_{\text{UV}}}, \quad (36)$$

where  $J_n$  and  $Y_n$  are Bessel functions of order  $n$  and  $p$  is the Euclidean momentum, and

$$b(p) = - \left. \frac{z \partial_z J_{\sqrt{-\epsilon}}(ipz) + \tilde{m}_b^2 J_{\sqrt{-\epsilon}}(ipz)}{z \partial_z Y_{\sqrt{-\epsilon}}(ipz) + \tilde{m}_b^2 Y_{\sqrt{-\epsilon}}(ipz)} \right|_{z=z_{\text{IR}}}. \quad (37)$$

- $\epsilon < 0$ : Let us take the limit  $\epsilon \rightarrow 0$  from inside the conformal window with  $M_q \neq 0$  such that  $z_{\text{IR}}$  is fixed at some finite value. The scalar-scalar correlator Eq. (36) defined at  $z_{\text{UV}} \rightarrow 0$  simplifies to

$$\Pi_S(p) = M_5 L \left[ 2 + \frac{2b(p)}{\pi + 2b(p)(\gamma + \ln(ipz_{\text{UV}}/2))} \right] + \dots, \quad (38)$$

where

$$b(p) = - \frac{ipz_{\text{IR}} J_1(ipz_{\text{IR}}) - \tilde{m}_b^2 J_0(ipz_{\text{IR}})}{ipz_{\text{IR}} Y_1(ipz_{\text{IR}}) - \tilde{m}_b^2 Y_0(ipz_{\text{IR}})}. \quad (39)$$

For large momentum  $pz_{\text{IR}} \gg 1$ , Eq. (38) gives

$$\Pi_S(p) \simeq M_5 L \left[ 2 + \frac{1}{\gamma + \ln(pz_{\text{UV}}/2)} \right]. \quad (40)$$

The origin of the logarithm is expected from the discussion in Sec. 2. The theory contains the marginal term  $f(\mu) \text{Tr}[\mathcal{O}_\Phi \mathcal{O}_\Phi]$  where  $f$  runs according to Eq. (3). For  $pz_{\text{UV}} \rightarrow 0$  the log-dependent term goes to zero and the theory enters into the conformal regime.

Therefore the mass spectrum of the scalars are not sensitive to  $\ln z_{\text{UV}}$  terms. Using the fact that a scalar-scalar correlator in a large- $N_c$  theory can also be written as a sum over

infinitely narrow resonances

$$\Pi_S(p) = \sum_{i=1}^{\infty} \frac{F_{S_i}^2 m_{S_i}^2}{p^2 + m_{S_i}^2}, \quad (41)$$

we can obtain the mass spectrum by looking at the poles of Eq. (38). Taking  $\tilde{m}_b^2 = 1$  we find that the lightest resonance, that we named as in QCD  $f_0$ , is given by  $m_{f_0} \simeq 1.26/z_{\text{IR}}$ , much lighter than the  $\rho$  meson mass that in the approximation that we are taking here is  $m_\rho \simeq 2.4/z_{\text{IR}}$ . In fact, we find that  $m_{f_0}/m_\rho < 1$  is true for any value of  $\tilde{m}_b^2 \geq 0$ .

The reason of why the lightest scalar meson is lighter than the  $\rho$  is tied to the fact that the mass of  $M_\Phi^2$  is taking at the conformal edge the lowest possible value ( $M_\Phi^2 L^2 \rightarrow -4$ ) [14]. We can see this analytically by taking the limit  $m_{S_i} z_{\text{IR}} \gg 1$ . We find

$$m_{S_i} \simeq \left(i - \frac{3}{4} + \frac{\sqrt{-\epsilon}}{2}\right) \frac{\pi}{z_{\text{IR}}}, \quad i = 1, 2, \dots, \quad (42)$$

that shows that the lightest state mass minimizes for  $\epsilon = 0$ . As we already said, this can also be understood from the CFT point of view. Close to the conformal lower edge the dimension of  $\mathcal{O}_\Phi = q\bar{q}$  takes the closest value to the unitarity bound ( $\text{Dim}[q\bar{q}] > 1$ ) where a scalar is expected to become massless since  $\mathcal{O}_\Phi$  decouples from the CFT [11].

- $\epsilon > 0$ : Let us now consider the limit  $\epsilon \rightarrow 0$  from outside the conformal window. We recall that we have to take this limit such that Eq. (29) is kept fixed. This leads to

$$\Pi_S(p) \simeq M_5 L \left[ 2 + \frac{2b(p)}{\pi + 2b(p)(\gamma + \ln(ipz_c/2) + \tilde{M}_q)} \right], \quad (43)$$

where  $\tilde{M}_q = M_q z_{\text{IR}}^2 / (L\phi_{\text{IR}}\tilde{m}_b^2)$ . Notice that it is now  $z_c \sim z_{\text{IR}}$  that regulate the logarithm and not  $z_{\text{UV}}$  as in the  $\epsilon < 0$  case. This means that the logarithmic breaking of conformal invariance remains at low-energies. For large values of  $M_q$  however this term tends to zero and Eq. (43) approaches Eq. (38). This was expected from the discussion in Sec. 2: the presence of a large  $M_q$  sets a mass gap to the theory much larger than the scale  $z_c$ ; the IR flow "stops" when the theory is (almost) a CFT, much before the coupling  $f(\mu)$  blows up. The theory in this case has to have the same behavior as that for  $\epsilon < 0$ .

The scalar meson masses are determined by the poles of Eq. (43). We get

$$b(m_{S_i}) = -\frac{\pi/2}{\gamma + \ln(m_{S_i} z_c/2) + \tilde{M}_q}. \quad (44)$$

Taking the approximation  $m_{S_i} z_{\text{IR}} \gg 1$  and using Eq. (30), we obtain

$$m_{S_i} \simeq \left(i - \frac{3}{4}\right) \frac{\pi}{z_{\text{IR}}} - \frac{\pi/2}{\gamma + \ln(m_{S_i} z_{\text{IR}}/2) + \frac{1}{\tilde{m}_b^2} + \tilde{M}_q} \frac{1}{z_{\text{IR}}}, \quad i = 1, 2, \dots. \quad (45)$$

Notice that the masses are sensitive to a logarithmic conformal breaking (there is no a simple scaling with  $1/z_{\text{IR}}$ ), different from the case  $\epsilon < 0$ . Nevertheless, as expected, Eq. (45) tends to Eq. (42) for  $M_q \rightarrow \infty$ .

The numerical results (with no approximations) for the masses of the lightest scalar singlet ( $f_0$ ) and adjoint ( $a_0$ ) are shown in Fig. 2. The masses are different at the two sides of the conformal transition due to the log terms discussed above. The dependence on  $M_q$  for  $\epsilon > 0$  is shown in Fig. 3. As  $M_q$  grows, the masses tend to the values for  $\epsilon < 0$  (hyperscaling case), shown as dashed lines.

### 4.3.2 Angular fluctuations: the pions

Let us finally comment on the angular fluctuations of  $\Phi$ , the pions. These are the only states sensitive to the UV-boundary condition and therefore the ones that clearly distinguish among the two limits towards the conformal edge. As explained above, for  $\epsilon > 0$  and  $M_q = 0$  the model shows spontaneous chiral symmetry breaking and we expect the pions to be massless. On the other side,  $\epsilon < 0$ , the chiral breaking is explicit (UV driven by  $M_q$ ) and the pions should have a mass as large as the other mesons, following hyperscaling Eq. (10). This is shown in Fig. 3. It is interesting to remark that we find  $m_\pi < m_{f_0}$  for any value of  $M_q$  and for any value of the parameters of the model.

## 4.4 Moving further inside the conformal window

As  $M_\Phi^2$  moves from  $-4$  to  $-3$ , corresponding to an increase of  $\text{Dim}[q\bar{q}]$  from 2 to 3, we are getting further inside the conformal window (see Fig. 1). We expect the scalar mesons to become heavier since we are moving away from the unitarity bound ( $\text{Dim}[q\bar{q}] > 1$ ).

On the other hand, the explicit chiral breaking is dictated by  $M_q$  whose dimension moves from 2 to 1. As a consequence, the profile of  $\phi$ , that grows as

$$\phi \sim M_q z^{\text{Dim}[M_q]}, \quad (46)$$

becomes flatter and spreads more into the  $\text{AdS}_5$  space. To keep  $F_\pi/m_\rho$  constant, the flatter the  $\phi$  profile, the smaller  $\phi_{\text{IR}}$  must be. This implies that the effect of  $\phi$  on the IR ( $z \sim z_{\text{IR}}$ ) becomes relatively weaker. Since the spectrum of resonances is determined by the fields at  $z \sim z_{\text{IR}}$ , we expect that they will notice less the chiral breaking driven by  $\phi$ . This is indeed seen in Fig. 2 where, as  $M_\Phi^2$  moves towards  $-3$ , we have  $m_{a_1} \rightarrow m_\rho$  and  $m_{a_0} \rightarrow m_{f_0} \rightarrow m_\pi$ . This behavior is also observed in lattice simulations as we will see below.

## 5 Comparison with lattice simulations

There are several lattice simulations of  $SU(3)$  QCD at large values of  $N_F$ . In [2, 4] lattice simulations for  $N_F = 8$  were provided, while results for  $N_F = 12$  were given in [5]. In [3] the value of  $N_F$  was effectively made to vary from 8 to 12 by varying the quark masses. In Fig. 4 we show the results of [3] for  $N_F = 3, 8$  and 12.

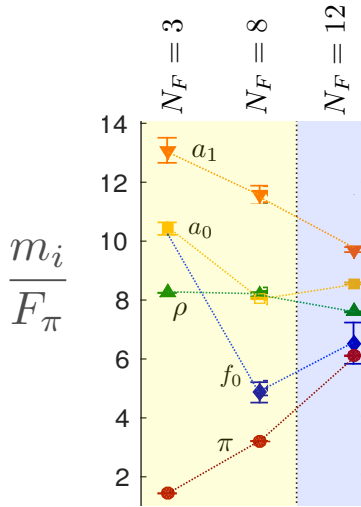


Figure 4: Lattice results from [3] for the QCD meson masses normalized to  $F_\pi$  for different values of  $N_F$ . See [3] for the values of the quark masses.

It is highly supported that QCD with  $N_F = 8$  flavors is outside the conformal window, while it is inside for  $N_F = 12$ . The main indication comes from the pion mass that it is seen to go to zero with  $M_q$  for  $N_F = 8$  and shows hyperscaling for  $N_F = 12$  [3], as it can be appreciated in Fig. 4. Therefore we can compare our results inside and outside the conformal window with those of lattice for  $N_F = 8$  and  $N_F = 12$  respectively.

Fig. 4 shows the following general features:

- The scalars are the lightest states for  $N_F = 8$  where we expect QCD to be outside (but close) to the conformal window.
- The chiral-breaking mass splittings diminish as  $N_F$  increases and we move inside the conformal window ( $m_{a_1} \rightarrow m_\rho$ ,  $m_{a_0} \rightarrow m_{f_0} \rightarrow m_\pi$ ).

These properties are quite close to the ones derived in our holographic model. Increasing  $N_F$  is equivalent to increasing  $M_{\mathbb{F}}^2$  in holographic models and Fig. 2 shows that chiral breaking effects become weaker. Also the scalar  $f_0$  is predicted to be light close to the conformal transition. Nevertheless, our holographic model also predicts a light radion/dilaton that was advocated in [14] to be associated with the lightest scalar seen in lattice simulation. Nevertheless, the radion/dilaton is predicted to be mostly a glueball whose mass is smooth as we cross the conformal transition (sky-blue line in Fig. 2). This is in contradiction with lattice results that seem to suggest that the lightest  $0^{++}$  scalar is a  $q\bar{q}$  meson, not a glueball, since its mass tends to  $m_\pi$  for large  $N_f$ . The light glueball present in our holographic model could be then a feature of the simple IR-brane setup that might be absent in more realistic holographic models. We leave this investigation for the future.

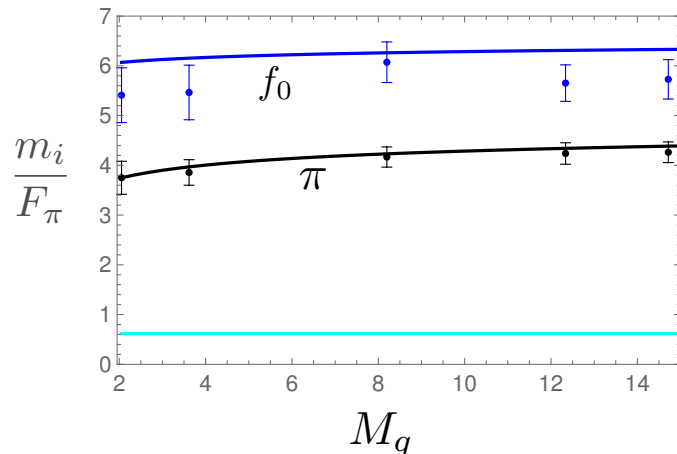


Figure 5: Predictions for meson masses normalized to  $F_\pi$  as a function of  $M_q$ . The sky-blue line corresponds to the dilaton/radion (glueball). Data points are lattice results from [22].

Another important feature derived from our analysis is the dependence of the meson masses with  $M_q$ , shown in Fig. 3. This property might offer an additional hint to the nature of the light scalar:  $q\bar{q}$  meson if its mass has a  $M_q$  dependence (see Eq. (45)), or a glueball if not. In Fig. 5 we show our predictions for the masses of  $f_0$ ,  $\pi$  and glueball (normalized to  $F_\pi$ ) as a function of  $M_q$ , and compare them with the lattice predictions of [22].<sup>8</sup> Unfortunately, at present lattice results are not accurate enough to clearly distinguish any dependence with  $M_q$ , with the exception of  $m_\pi$ . Fig. 5 however seems to slightly favor  $f_0$  as the lattice  $0^{++}$  state in front of a glueball state.

## 6 Conclusions

We have analyzed how the physical properties of a system change when approaches a conformal transition from both sides of the conformal edge. The derived properties seem to be generic for large- $N_c$  models where the conformal transition occurs by the merging of an IR and a UV fixed point. We have obtained the following features:

- The dilaton (mostly a glueball) is light at both sides of the conformal transition, showing that has nothing to do with the spontaneous breaking of conformal invariance. This is very different from the pion that is massless outside the conformal window but massive inside due respectively to the spontaneous and explicit breaking of the chiral symmetry.
- The scalar meson  $f_0$  (mostly a  $\bar{q}q$  state) is light close to the conformal edge, being lighter when approaching it from outside the conformal window than from inside—see Fig. 3. Its

<sup>8</sup>We have fitted the lowest value of  $m_\pi/F_\pi$  in [22] to our prediction in order to normalize our  $M_q$  with that in [22].



mass shows a dependence with  $M_q$  predicted as in Eq. (45) that can be parametrized as

$$\frac{m_{f_0}}{m_\rho} = \frac{a_{f_0}}{a_\rho} - \frac{\alpha_1}{\alpha_2 \ln \frac{m_{f_0}}{m_\rho} + M_q}, \quad (47)$$

where  $a_i$  are the hyperscaling values (Eq. (10)) and  $\alpha_i$  are constants.

- Our model predicts  $m_\pi < m_{f_0}$  inside the conformal window.
- Spin-1 meson masses as well as  $F_\pi$  are practically smooth across the conformal transition and independent of  $M_q$  as shown in Fig. 3.
- Chiral symmetry breaking effects become smaller as we move further inside the conformal window, i.e.,  $m_{a_1} \rightarrow m_\rho$  and  $m_{a_0} \rightarrow m_{f_0} \rightarrow m_\pi$ . This is because the dimension of  $M_q$ , responsible for the chiral and conformal symmetry breaking, decreases.

Most of these generic properties seem to be followed by QCD as we increase  $N_F$  as lattice results show in Fig. 4.

Models close to the conformal transition can also be useful for physics beyond the SM [14]. In particular, if this phase transition occurs in the early universe, a supercooled epoch can generate interesting signal [23, 24]. These applications are left for the future.

## Acknowledgements

We would like to thank Oriol Pujolas for collaborating at the early stages of this work. LS also thanks Leandro Da Rold for useful correspondence. The authors acknowledge support from the Departament de Recerca i Universitats from Generalitat de Catalunya to the Grup de Recerca "Grup de Física Teòrica UAB/IFAE" (Codi: 2021 SGR 00649). This work has also been supported by the research grant PID2020-115845GB-I00/AEI/10.13039/501100011033.

## References

- [1] D. B. Kaplan, J. W. Lee, D. T. Son and M. A. Stephanov, Phys. Rev. D **80** (2009) 125005.
- [2] Y. Aoki *et al.* [LatKMI Collaboration], Phys. Rev. D **96** (2017) no.1, 014508; Phys. Rev. D **89** (2014) 111502.
- [3] R. C. Brower, A. Hasenfratz, C. Rebbi, E. Weinberg and O. Witzel, Phys. Rev. D **93** (2016) no.7, 075028; A. Hasenfratz, C. Rebbi and O. Witzel, Phys. Lett. B **773** (2017), 86-90.
- [4] T. Appelquist *et al.* [Lattice Strong Dynamics Collaboration], Phys. Rev. D **93** (2016) no.11, 114514; Phys. Rev. D **99** (2019) no.1, 014509.

- [5] Z. Fodor, K. Holland, J. Kuti, D. Nogradi, C. Schroeder, K. Holland, J. Kuti, D. Nogradi and C. Schroeder, Phys. Lett. B **703** (2011), 348-358; Y. Aoki, T. Aoyama, M. Kurachi, T. Maskawa, K. i. Nagai, H. Ohki, A. Shibata, K. Yamawaki and T. Yamazaki, Phys. Rev. D **86** (2012), 054506; Y. Aoki *et al.* [LatKMI], Phys. Rev. Lett. **111** (2013) no.16, 162001.
- [6] E. Pomoni and L. Rastelli, JHEP **0904** (2009) 020.
- [7] V. Gorbenko, S. Rychkov and B. Zan, JHEP **1810** (2018) 108.
- [8] M. Golterman and Y. Shamir, Phys. Rev. D **94** (2016) no.5, 054502; Phys. Rev. D **95** (2017) no.1, 016003; Phys. Rev. D **98** (2018) no.5, 056025; Phys. Rev. D **102** (2020), 114507; M. Golterman, E. T. Neil and Y. Shamir, Phys. Rev. D **102** (2020) no.3, 034515; A. Freeman, M. Golterman and Y. Shamir, Phys. Rev. D **108** (2023) no.7, 074506;
- [9] T. Appelquist, J. Ingoldby and M. Piai, JHEP **07** (2017), 035; JHEP **03** (2018), 039; Phys. Rev. D **101** (2020) no.7, 075025 Phys. Rev. Lett. **126** (2021) no.19, 191804; Nucl. Phys. B **983** (2022), 115930; Universe **9** (2023) no.1, 10.
- [10] J. M. Maldacena, Adv. Theor. Math. Phys. **2** (1998) 231; S. S. Gubser, I. R. Klebanov and A. M. Polyakov, Phys. Lett. B **428** (1998) 105; E. Witten, Adv. Theor. Math. Phys. **2** (1998) 253.
- [11] See for example, B. Grinstein, K. A. Intriligator and I. Z. Rothstein, Phys. Lett. B **662** (2008) 367.
- [12] A. G. Cohen and H. Georgi, Nucl. Phys. B **314** (1989), 7-24.
- [13] R. Zwicky, [arXiv:2306.06752 [hep-ph]].
- [14] A. Pomarol, O. Pujolas and L. Salas, JHEP **10** (2019), 202.
- [15] J. Albert and L. Rastelli, JHEP **08** (2022), 151.
- [16] C. Fernandez, A. Pomarol, F. Riva and F. Sciotti, JHEP **06** (2023), 094; T. Ma, A. Pomarol and F. Sciotti, JHEP **11** (2023), 176.
- [17] D. Kutasov, J. Lin and A. Parnachev, Nucl. Phys. B **858** (2012) 155; Nucl. Phys. B **863** (2012) 361.
- [18] A. F. Faedo, C. Hoyos, D. Mateos and J. G. Subils, Phys. Rev. Lett. **124** (2020) no.16, 161601; JHEP **10** (2021), 246.
- [19] E. Witten, hep-th/0112258.
- [20] L. Vecchi, Phys. Rev. D **82** (2010) 045013 [arXiv:1004.2063 [hep-th]]; D. Elander and M. Piai, JHEP **1101** (2011) 026; S. P. Kumar, D. Mateos, A. Paredes and M. Piai, JHEP **1105** (2011) 008; M. Jarvinen and E. Kiritsis, JHEP **1203** (2012) 002; N. Evans and K. Tuominen, Phys. Rev. D **87** (2013) no.8, 086003; J. Erdmenger, N. Evans and M. Scott, Phys. Rev. D **91** (2015) no.8, 085004; M. Jarvinen, JHEP **1507** (2015) 033; D. Elander,

R. Lawrance and M. Piai, Nucl. Phys. B **897** (2015) 583; N. Evans, P. Jones and M. Scott, Phys. Rev. D **92** (2015) no.10, 106003; D. Arean, I. Iatrakis, M. Jarvinen and E. Kiritsis, Phys. Rev. D **96** (2017) no.2, 026001; K. Bitaghsir Fadafan, W. Clemens and N. Evans, Phys. Rev. D **98** (2018) no.6, 066015; D. Elander, M. Piai and J. Roughley, JHEP **1902** (2019) 101; Y. Buyukdag, Phys. Rev. D **102** (2020) no.10, 106018; D. Elander, M. Frigerio, M. Knecht and J. L. Kneur, JHEP **03** (2021), 182; D. Elander, M. Piai and J. Roughley, JHEP **06** (2020), 177 [erratum: JHEP **12** (2020), 109]; Phys. Rev. D **103** (2021), 106018; Phys. Rev. D **103** (2021) no.4, 046009; Phys. Rev. D **104** (2021) no.4, 046003; D. Elander, A. Fatemiabhari and M. Piai, Phys. Rev. D **107** (2023) no.11, 115021; J. Cruz Rojas, D. K. Hong, S. H. Im and M. Järvinen, JHEP **05** (2023), 204; D. Elander, A. Fatemiabhari and M. Piai, Phys. Rev. D **108** (2023) no.1, 015021.

[21] L. Da Rold and A. Pomarol, Nucl. Phys. B **721** (2005) 79; JHEP **0601** (2006) 157.

[22] T. Appelquist *et al.* [LSD], [arXiv:2305.03665 [hep-lat]].

[23] P. Baratella, A. Pomarol and F. Rompineve, JHEP **1903** (2019) 100.

[24] C. Csáki, M. Geller, Z. Heller-Algazi and A. Ismail, JHEP **06** (2023), 202.